The lattice dynamics of gallium phosphide

J. Phys. C: Solid State Phys., Vol. 12, 1979. Printed in Great Britain. © 1979

The lattice dynamics of gallium phosphide

P H Borcherds†, K Kunc‡, G F Alfrey§, R L Hall†

† Department of Physics, University of Birmingham B15 2TT, UK
‡ Laboratoire de Physique des Solides, Universite de Paris VI, France
§ Department of Space Research, University of Birmingham, UK

Received 9 April 1979

Abstract. The phonon frequencies of gallium phosphide were measured along the Δ-, Σ-, Λ- and Z-lines and a valence–force-field overlap shell model, which reproduces the considerable dispersion observed along the Z line, is used to explain them.

1. Introduction

Gallium phosphide is one of the III–V semiconductors which crystallise into the zincblende structure: this is one of the simplest acentric crystal structures and is therefore a very suitable system to study. That the III–V semiconductors are of technological importance provides a complementary reason for studying them.

A considerable effort has already been made to understand the lattice dynamics of crystals with the zincblende structure, both experimentally, using mainly inelastic neutron scattering, and theoretically, using a variety of models (Price *et al* 1971, Farr *et al* 1975, Rowe *et al* 1974, Borcherds and Kunc 1978).

Since the development of the triple-axis neutron spectrometer (Brockhouse 1961) most measurements of phonon energies have been carried out on these instruments. This technique has the advantage that the wavevector of the phonon whose energy is to be measured may be predetermined and, in general, only those phonons whose wavevectors lie along lines of symmetry are then measured. In the case of cubic crystals the three chief lines of symmetry are ⟨100⟩ ⟨110⟩ and ⟨111⟩ (Δ, Σ and Λ respectively).

It is particularly easy to calculate the phonon energies for these lines, since the dynamical matrix (which is a 6 × 6 Hermitian matrix) can be broken down into smaller matrices (usually 2 × 2) for these lines, and can thus be diagonalised more easily. This point is now of less importance than previously because of the availability of efficient subroutines for diagonalising Hermitian matrices, e.g. ECO7C from the Harwell subroutine library. It is also particularly easy to display experimental results when the phonon wavevectors lie along symmetry lines: the sections through the dispersion surface become the familiar dispersion curves.

The above three special lines sample a comparatively small fraction of the Brillouin zone, (particularly so well away from the zone centre). Another line which is comparatively easy to study and interpret is the Z-line, which lies across the diagonals of the square faces of the Brillouin zone. The W-point, at the corners of the faces, is of some importance. first of all because, owing to its high multiplicity, it makes a large

contribution to the density of states, and secondly, because it is found that in the important ternary compounds related to the zincblende structure, two of the W-points fold into the zone centre and become Γ-points: a knowledge of the phonons near the W-points in the zincblende structure will assist our understanding of the ternary materials. It is difficult to carry out such measurements on the ternary compounds directly, since suitable single crystals are unavailable.

2. Experimental details

The phonon dispersion curves of gallium phosphide were first measured by Yarnell *et al* (1968). They used a composite 'single' crystal built up from 36 aligned platelets.

We have repeated their measurements using a high-purity single crystal 35 mm diameter and 15 mm thick. Its carrier concentration at room temperature is $1{\cdot}1 \times 10^{17}$ cm^{-3} (n-type). The crystal was cut from a nearly circularly cylindrical ingot, and has a $\langle 111 \rangle$ axis normal to its flat face. This shape, with a $\langle 1\bar{1}0 \rangle$ axis vertical, is particularly suitable for studying the phonons along Δ, Σ and Λ (Borcherds *et al* 1975), but in order to measure phonons along Z the crystal had to be mounted with its $\langle 001 \rangle$ axis vertical.

By a suitable choice of the scattering vector it is possible in this configuration to measure all six phonon branches along the Z-line. It is also possible to measure the truly transverse modes along Σ, the Σ_2 modes which are not accessible with the $\langle 110 \rangle$ axis vertical.

The measurements were carried out on the triple-axis spectrometer on the DIDO reactor at Harwell, using an aluminium monochromator and a pyrolytic graphite (0002) analyser. For measuring the acoustic phonons we used the $\{111\}$ reflection from the aluminium ($\lambda = 1{\cdot}623$ Å), and for the optic phonons, the $\{220\}$ reflection from aluminium ($\lambda = 1{\cdot}000$ Å) was used.

The measured phonon frequencies are given in table 1, and are in good agreement with those obtained by Yarnell *et al*, as can be seen in figure 1. In that figure we show also the results of calculations described below.

3. Lattice dynamics models

It has been found necessary to use a shell model with short-range forces between second neighbours in order to explain the dispersion curves of crystals with the zincblende structure. Simpler models, i.e. the rigid-ion model and a model with short-range forces between nearest neighbours only, are quite inadequate. The second-neighbour shell model, in its most general form, has 37 independently adjustable parameters; too many both for aesthetic and for practical reasons.

The second-neighbour shell model for the zincblende structure was first used by Dolling and Waugh (1965) for GaAs. In order to reduce the number of independent parameters they introduced various arbitrary relationships and in this way obtained a model with 14 independent parameters. This 14-parameter model has been used by several other workers and gives a good fit to the dispersion curves.

At about the same time that the 14-parameter model was being developed, Musgrave and Pople (1961) introduced the valence-force-field (VFF) model. In this model the short-range forces act between nearest and second-nearest neighbours, but are postulated to

Table 1. Phonon frequencies in GaP (THz).

(*a*) Wavevector along Δ. (00ξ)

ξ	TA	LA	TO	LO
0(Γ)	0	0		12·25 ± 0·05
0·1	0·88 ± 0·02			12·2 ± 0·10
0·2	1·43 ± 0·02	2·3 ± 0·05	10·75 ± 0·3	11·9 ± 0·4
0·3	1·98 ± 0·02	3·30 ± 0·05		
0·4	2·40 ± 0·02	4·25 ± 0·05		
0·5	2·75 ± 0·02	5·0 ± 0·3	10·7 ± 0·4	11·75 ± 0·4
0·6	2·95 ± 0·02	5·7 ± 0·2		
0·7	3·10 ± 0·05			
0·8		7·18 ± 0·3	10·8 ± 0·2	11·3 ± 0·5
0·9				
1·0(X)	3·13 ± 0·15	7·5 ± 0·4	10·65 ± 0·5	11·0 ± 0·3

(*b*) Wavevector along Σ (0$\xi\xi$)

	TA	A_I	A_{II}	TO	O_I	O_{II}
0(Γ)	0	0	0			12·25 ± 0·05
0·1		1·06 ± 0·02	1·73 ± 0·05	10·7 ± 0·4		11·8 ± 0·1
0·2		2·15 ± 0·05	3·17 ± 0·05	10·6 ± 0·3		
0·3	2·11 ± 0·1	2·80 ± 0·05	4·35 ± 0·1	10·5 ± 0·5		
0·4	2·58 ± 0·1	3·40 ± 0·05		10·6 ± 0·3		
0·5	2·90 ± 0·1	3·92 ± 0·05		10·65 ± 0·4		
0·6	3·05 ± 0·1	4·25 ± 0·05		10·5 ± 0·4		
0·7	3·17 ± 0·2	4·70 ± 0·1				
0·75	3·15 ± 0·2			10·5 ± 0·3		
0·8	3·15 ± 0·15			10·6 ± 0·5		
0·9						
1·0(X)	3·13 ± 0·15	3·13 ± 0·15	7·5 ± 0·14	10·65 ± 0·5	10·65 ± 0·5	11·0 ± 0·3

(*c*) Wavevector along Λ ($\xi\xi\xi$)

	TA	LA	TO	LO
0(Γ)	0	0		12·25
0·1	1·05 ± 0·05		10·6 ± 0·2	12·0 ± 0·1
0·2	1·80 ± 0·02	4·00 ± 0·05	10·75 ± 0·2	
0·3	2·25 ± 0·02	5·55 ± 0·1		
0·4	2·40 ± 0·05		10·9 ± 0·05	12·25 ± 0·1
0·5(L)	2·50 ± 0·05		10·6 ± 0·2	12·16 ± 0·05

(*d*) Wavevector along Z (1ξ0)

	A_I	A_{II}	A_{III}	O_I	O_{II}	O_{III}
0(X)	3·13 ± 0·15	3·13 ± 0·15	7·5 ± 0·4	10·65 ± 0·5	10·65 ± 0·5	11·0 ± 0·3
0·1	3·15 ± 0·2	3·23 ± 0·2	7·4 ± 0·4			
0·2	3·44 ± 0·1	3·55 ± 0·2	7·2 ± 0·2	10·5 ± 0·7		
0·3	3·50 ± 0·1	4·0 ± 0·1	6·9 ± 0·2			
0·4	3·65 ± 0·15	4·25 ± 0·1	6·5 ± 0·3	10·7 ± 0·4		
0·5(W)	3·70 ± 0·1	4·60 ± 0·1	6·4 ± 0·5	10·8 ± 0·5		

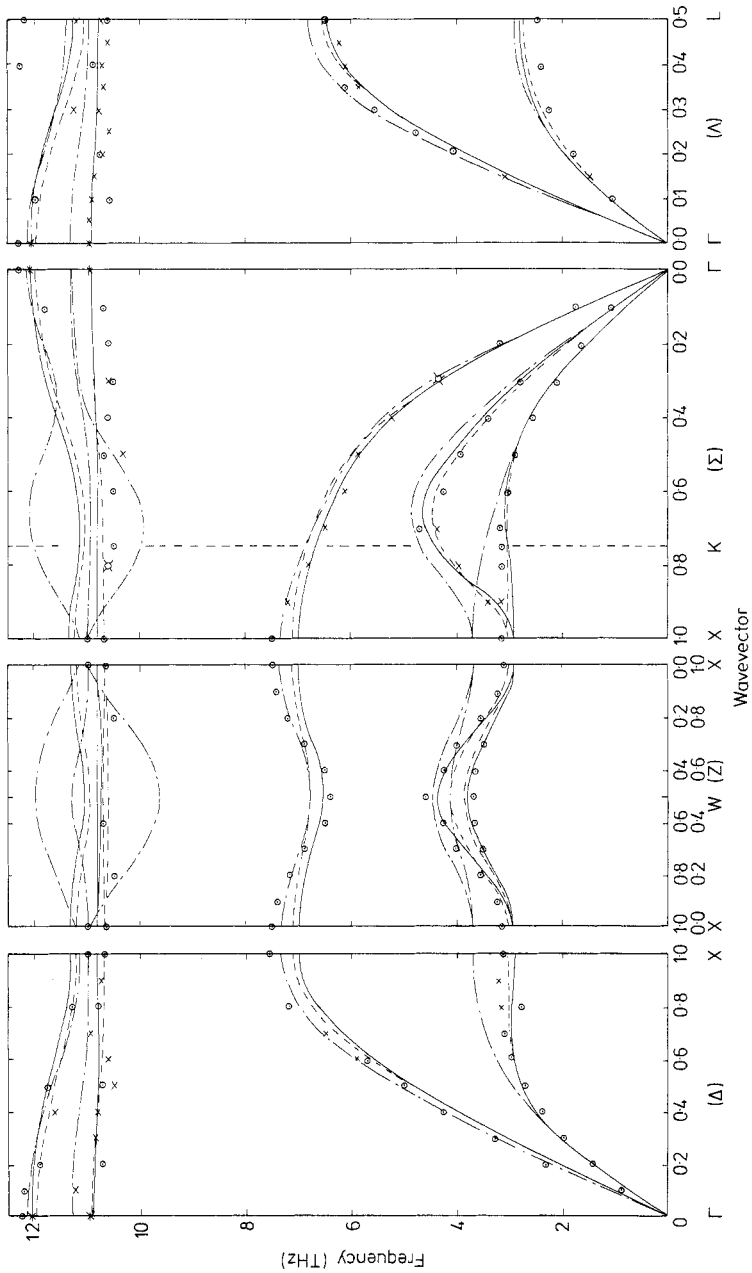

Figure 1. Phonon dispersion curves for gallium phosphide. Full curves: best fit OVSM calculations (table 2, model B); broken curves: OVSM fit of Kunc and Bilz (1976a) (table 2, model A); chain curves: '14-parameter model' fit (J L Yarnell, private communication); ○: experimental points (this paper); ×: experimental points (Yarnell *et al* 1968).

be either bond-stretching or bond-bending: this restriction significantly reduces the number of parameters and is also physically plausible. If, in addition, we postulate that the short-range forces act only between the shells, again a plausible assumption, we obtain a model with only 10 adjustable parameters.

Bilz *et al* (1975) have shown that it is physically plausible to require that the shell of the cation should be positively charged: the valence and force-field model satisfying this criterion is known as the overlap shell model (OVSM).

Kunc and Bilz (1976a) examined a number of published lattice dynamics models for materials with the zincblende structure. For each model they calculated the Raman spectrum (which depends on the phonon polarisation vectors) and were able to show that most published models were unsatisfactory in this respect. The only ones they found to be satisfactory were the OVSM models of Vagelatos *et al* (1974) for ZnS and ZnTe.

4. Calculations

Even when the decision has been taken to consider only the valence-force-field overlap shell model, there is still a virtually infinite number of models, i.e. sets of parameters which will all fit the experimental phonon frequencies equally well. To restrict the choice further, we make the physically plausible assumptions that the charges on the ions should be (i) a few electronic charges equal to or less than the valence charge, to take account of covalence bonding, and (ii) of the appropriate sign, to take account of ionic bonding.

The models of Vagelatos *et al* (1974) for ZnS and ZnTe, which are based on the above assumptions, give reasonably good Raman spectra (Kunc and Bilz 1976a). There is thus some merit in trying to find similar models for other materials with the zincblende structure. Kunc and Bilz (1976a) did this, using a constrained least-squares fitting procedure. Since we have used the same procedure, we shall describe it fully.

Zinc and gallium, and also phosphorus and sulphur, are consecutive elements in the periodic table so it may be expected that the model parameters for GaP will be similar to those for ZnS. As a first step in fitting the GaP data, phonon frequencies were calculated using the ZnS model, but with atomic masses and lattice constants altered to the values for GaP.

The calculated and experimental values were compared and their average ratio calculated. As a second step in obtaining a suitable model, all the force parameters were scaled by the square of this ratio, while the charge terms were scaled by the ratio. This gave a model whose phonon frequencies were in rough agreement with experiment.

Constrained least-squares fitting was used in order to improve the model: strict limits, initially $\pm 10\%$, were placed on each parameter and a least-squares fitting program (MINUIT: James and Roos 1975) was used. For some parameters the above limits were too tight, and these were relaxed as necessary.

Kunc and Bilz carried out this procedure for GaP using the data of Yarnell *et al*, and we present their model in table 2 (model A). We used the model of Kunc and Bilz for GaP as the starting point for our model. which is shown in table 2 (model B), and this also takes into account the extra measurements reported above, particularly those along the Z-line.

4.1. Dispersion along the Z-line

The earliest discussion of phonon frequencies along the Z-line for the zincblende

Table 2. Parameters of OVSM for GaP. The force terms are in units of $e^2/4a^3$ and the charge terms are in electron units.

	Model A (Kunc & Bilz)	Model B (this paper)
λ	47·5	45·0
k_σ	−1·15	−1·15
$k_{\sigma'}$	−0·310	−0·206
kr_θ	4·61	4·61
$kr_{\theta'}$	−7·06	−7·83
Z_1	2·00	2·03
Y_1	6·03	5·47
Y_2	−1·87	−1·97
k_1	371·2	350·0
k_2	82·0	87·0

structure (Johnson 1965) used a nearest-neighbour rigid-ion model, which predicts that the dispersion curves are quite flat, with the consequence that there are two pairs of degenerate branches, corresponding to the degeneracy of the transverse modes at the X-point.

It is only for nearest-neighbour forces that the curves are flat; second-neighbour forces not only introduce dispersion, but also lift the degeneracy of the branches.

It is well known (from the diatomic linear chain) that at the Brillouin zone boundary (X-point) the distinction between the optic and acoustic branches in the zincblende structure is that the motion of the two sublattices is decoupled and that one sublattice moves, while the other is stationary, and vice versa. By examining the polarisation vectors of the phonons it can be seen that the atomic motions of the two sublattices are decoupled the whole way along Z.

There are three modes which for wavevector $(\zeta, 1, 0)$ have the polarisation vector

$$\xi = (a_{1x}; a_{2y} + ia_{2z})$$

and three with

$$\xi = (a_{1y} + ia_{1z}; a_{2x}).$$

In all cases the atoms on one sublattice execute linear motion along the x direction for such a wavevector, while those on the other execute elliptic motion in the y–z plane. In table 3 we show the polarisation vectors for all six branches as for wavevector (0·25, 1, 0).

At the point W the ellipses open out into circles, and for two of the branches (I and IV in the notation of table 3) one of the sublattices is stationary. On approaching the X-point the ellipses close down into lines and one of the sublattices is stationary for each branch as already mentioned.

5. Results and discussion

The phonon dispersion curves are shown in figure 1. The 10-parameter OVSM gives a slightly better overall fit to the experimental data than does the '14-parameter' model, as can be seen from the figure.

The major observable difference between the dispersion curves calculated from the

two types of models is that there is far more dispersion predicted by the 14-parameter model for some optic branches along Σ and Z. The OVSM model predicts flatter branches, and seems to be in better agreement with the data. It is unfortunate that the data on these optic phonons is so sparse, but they are remarkably difficult to measure. This may be because they are inherently elliptically polarised as discussed in the previous section,

Table 3. Polarisation vectors for the wavevector (0·25, 1, 0). The vectors are normalised so that $\Sigma\xi_i^2 = 1$. The atomic motions are given by $x_i = \xi_i/\sqrt{M_i}$.

Branch	Frequency (THz)	a_{1x}	a_{1y}	a_{1z}	a_{2x}	a_{2y}	a_{2z}
I	11·20	0·01				−0·96	0·29i
II	10·81		0·09	−0·19i	0·98		
III	10·77	0·18				0·29	0·94i
IV	6·81		0·96	0·27i	−0·04		
V	3·66		0·26	−0·94i	−0·20		
VI	3·38	0·98				−0·04	−0·18i

and one cannot therefore select a scattering geometry in which only one of two nearly degenerate phonons is contributing to the peak. The effect is twofold: less neutrons are scattered by each phonon, while at the same time, both phonons are scattering, thus widening the apparent 'peak' and making it more difficult to detect.

6. Conclusion

We have demonstrated that the significant dispersion observed along the Z-line in the zincblende structure can be adequately modelled by the valence–force-field overlap shell model. The original parameters used by Kunc and Bilz (1976b), (model A) did not produce a good fit to the Z-line data, but with the slight shift of parameters (model B), shown in table 2, we obtained a good fit for all the experimental data. As pointed out by Bilz *et al* (1975), a fit to within a few per cent is all that should be expected of a harmonic lattice dynamics model, and this we have obtained. Further improvement may follow from the development of an anharmonic model, but a considerable amount of theoretical development is still needed.

Acknowledgments

We wish to thank D H Saunderson, D H C Harris and N Hance, all of AERE for their assistance with the experimental work; M Balkanski, of the University of Paris VI for his interest and hospitality during the calculations; and H Bilz of the Max Planck Institute, Stuttgart and H Montgomery of the University of Edinburgh for drawing to our attention the importance of the Z-line. This work has been supported by the Science Research Council.

References

Bilz H, Buchanan M, Fischer K, Haberkorn R and Schröder U 1975 *Solid St. Commun.* **16** 1023–6
Borcherds P H, Alfrey G F, Saunderson D H and Woods A D B 1975 *J. Phys. C: Solid St. Phys.* **8** 2022–30

Borcherds P H and Kunc K 1978 *J. Phys. C: Solid St. Phys.* **11** 4145–55
Brockhouse B N 1961 *Inelastic scattering of neutrons in solids and liquids* (Vienna: IAEA) p 113
Dolling G and Waugh J L T 1965 *J. Phys. Chem. Solids. Suppl.* **1** 19–32
Farr M K, Traylor J G and Sinha S K 1975 *Phys. Rev.* B **11** 1587–94
James F and Roos M 1975 *Comput. Phys. Commun.* **10** 343–67
Johnson F A, 1965, *Prog. Semicond.* **9** 179–235
Kunc K and Bilz H 1976a *Proc. Conf. Neutron Scattering Gatlinburg* (ed Moon) 195–201
—— 1976b *Solid St. Commun.* **19** 1027–30
Musgrave M J P and Pople J A 1961 *Proc. R. Soc.* A **268** 474–84
Price D L, Rowe J M and Nicklow R M 1971 *Phys. Rev.* B **3** 1268–79
Rowe J M, Nicklow R M, Price D L and Zanio K 1974 *Phys. Rev.* B **10** 671–5
Vagelatos N, Wehe D and King J S 1974 *J. Chem. Phys.* **60** 3613–8
Yarnell J L, Warren J L and Wenzel R G 1968 *Neutron inelastic scattering* vol I (Vienna: IAEA) pp 301–13